Morphing Contact Representations of Graphs

Patrizio Angelini
University of Tübingen, Tübingen, Germany
angelini@informatik.uni-tuebingen.de

Steven Chaplick
University of Würzburg, Würzburg, Germany
steven.chaplick@uni-wuerzburg.de

Sabine Cornelsen
University of Konstanz, Konstanz, Germany
sabine.cornelsen@uni-konstanz.de

Giordano Da Lozzo
Roma Tre University, Rome, Italy
giordano.dalozzo@uniroma3.it

Vincenzo Roselli
Roma Tre University, Rome, Italy
vincenzo.roselli@uniroma3.it

Abstract

We consider the problem of morphing between contact representations of a plane graph. In a contact representation of a plane graph, vertices are realized by internally disjoint elements from a family of connected geometric objects. Two such elements touch if and only if their corresponding vertices are adjacent. These touchings also induce the same embedding as in the graph. In a morph between two contact representations we insist that at each time step (continuously throughout the morph) we have a contact representation of the same type.

We focus on the case when the geometric objects are triangles that are the lower-right half of axis-parallel rectangles. Such RT-representations exist for every plane graph and right triangles are one of the simplest families of shapes supporting this property. Thus, they provide a natural case to study regarding morphs of contact representations of plane graphs.

We study piecewise linear morphs, where each step is a linear morph moving the endpoints of each triangle at constant speed along straight-line trajectories. We provide a polynomial-time algorithm that decides whether there is a piecewise linear morph between two RT-representations of a plane triangulation, and, if so, computes a morph with a quadratic number of linear morphs. As a direct consequence, we obtain that for 4-connected plane triangulations there is a morph between every pair of RT-representations where the "top-most" triangle in both representations corresponds to the same vertex. This shows that the realization space of such RT-representations of any 4-connected plane triangulation forms a connected set.

2012 ACM Subject Classification Theory of computation → Computational geometry; Mathematics of computing → Graph algorithms

Keywords and phrases Contact representations, Triangulations, Planar morphs, Schnyder woods

Digital Object Identifier 10.4230/LIPIcs.SoCG.2019.10

Related Version A full version of the paper [5] is available at `https://arxiv.org/abs/1903.07595`.

Funding Work supported by DFG grant Ka812/17-1 and by MIUR-DAAD Joint Mobility Program n.57397196 (Angelini), by DFG grant WO 758/11-1 (Chaplick), and by MIUR Project "MODE" under PRIN 20157EFM5C, by MIUR Project "AHeAD" under PRIN 20174LF3T8, by MIUR-DAAD JMP N° 34120, and by H2020-MSCA-RISE project 734922 – "CONNECT" (Da Lozzo and Roselli).

Acknowledgements This work began at the Graph and Network Visualization Workshop (GNV'18) in Heiligkreuztal. We thank S. Felsner, N. Heinsohn, and A. Lubiw for interesting discussions.

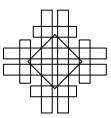

1 Introduction

We consider the morphing problem from the perspective of geometric representations of graphs. While a lot of work has been done to understand how to planarly morph the standard *node-link* diagrams[1] of plane graphs[2] and to "rigidly" morph[3] configurations of geometric objects, comparatively little has been explicitly done regarding (non-rigid) morphing of alternative representations of planar graphs, e.g., contact systems of geometric objects such as disks or triangles. In this case, the planarity constraint translates into the requirement of continuously maintaining a representation of the appropriate type throughout the morph.

More formally, let $\mathcal{F}$ be a family of geometric objects homeomorphic to a disk. An *$\mathcal{F}$-contact representation* of a plane graph G maps vertices to internally disjoint elements of $\mathcal{F}$. We denote the geometric object representing a vertex v by $\Delta(v)$. Objects $\Delta(v)$ and $\Delta(w)$ touch if and only if $\{v, w\}$ is an edge. The contact system of the objects must induce the same faces and outer face as in G. A *morph* between two $\mathcal{F}$-contact representations R_0 and R_1 of a plane graph G is a continuously changing family of $\mathcal{F}$-contact representations R_t of G indexed by time $t \in [0, 1]$. An implication of the existence of morphs between any two representations of the same type is that the topological space defined by such representations is connected. We are interested in elementary morphs, and in particular in *linear morphs*, where the boundary points of the geometric objects move at constant speed along straight-line trajectories from their starting to their ending position. A *piecewise linear morph of length ℓ* between two $\mathcal{F}$-contact representations R_1 and $R_{\ell+1}$ of a plane graph G is a sequence $\langle R_1, \ldots, R_{\ell+1}\rangle$ of $\mathcal{F}$-contact representations of G such that $\langle R_i, R_{i+1}\rangle$ is a linear morph, for $i = 1, \ldots, \ell$. For a background on the mathematical aspects of morphing, see, e.g., [3].

Morphs of Node-Link Diagrams. Fáry's theorem tells us that every plane graph has a node-link diagram where the edges are mapped to line segments. Of course, for a given plane graph G, there can be many such node-link diagrams of G, and the goal of the work in planar morphing is to study how (efficiently) one can create a smooth (animated) transition from one such node-link diagram to another while maintaining planarity. Already in the 1940's Cairns [17] proved that, for plane triangulations, planar morphs exist between any pair of such node-link diagrams. However, the construction involved exponentially-many morphing steps. Floater and Gotsman [29], and Gotsman and Surazhsky [31, 39] gave a different approach via Tutte's graph drawing algorithm [42], but this involves non-linear trajectories of unbounded complexity. Thomassen [40] and Aranov et al. [10] independently showed that two node-link diagrams of the same plane graph have a *compatible triangulation*[4] thereby lifting Cairns' result to plane graphs. Of particular interest is the study of *linear morphs*, where each vertex moves at a uniform speed along a straight-line. After several intermediate results to improve the complexity of the morphs [2, 6] and to remove the necessity of computing compatible triangulations [8], the current state of the art [1] is that there is a planar morph between any pair of node-link diagrams of any n-vertex plane graph using $\theta(n)$ linear steps. Planar morphs of other specialized plane node-link diagrams have also been considered, e.g., planar orthogonal drawings [13, 43], convex drawings [7], upward planar drawings [21], and so-called *Schnyder drawings* [12]. In this latter result the lattice structure of all Schnyder

[1] where vertices are represented as points and edges as non-crossing curves
[2] the set of faces and the outer face are fixed
[3] scaling the objects is not allowed, e.g., as in *bar-joint* systems [35] or in *body-hinge* systems [14, 19, 24]
[4] i.e., a way to triangulate both diagrams to produce the same plane triangulation

woods of a plane triangulation [15, 25] is exploited in order to obtain a sequence of linear morphs within a grid of quadratic size. Finally, planar morphs on the surface of a sphere [33] and in three dimensions have been investigated [11].

Morphs of Contact Representations. Similar to Fáry's theorem, the well-known Koebe-Andreev-Thurston theorem [4, 34] states that every plane graph G has a *coin* representation, i.e. an $\mathcal{F}$-contact representation where $\mathcal{F}$ is the set of all disks. Additionally, for the case of 3-connected plane graphs, such coin representations of G are unique up to *Möbius transformations* [16] – see [27] for a modern treatment. There has been a lot of work on how to intuitively understand and animate such transformations (see, e.g., the work of Arnold and Rogness [9]), i.e., for our context, how to morph between two coin representations. Of course, ambiguity remains regarding how to formalize the complexity of such morphs. In particular, this connection to Möbius transformations appears to indicate that a theory of piecewise linear morphing for coin representations would be quite limited.

For this reason, we instead focus on contact representations of convex polygons. These shapes still allow for representing all plane triangulations, as a direct consequence of the Koebe-Andreev-Thurston theorem, but are more amenable to piecewise linear morphs, where the linearity is defined on the trajectories of the corners. De Fraysseix et al. [23] showed that every plane graph G has a contact representation by triangles, and observed that these triangle-contact representations correspond to the 3-orientations (i.e., the *Schnyder woods*) of G. Schrenzenmaier [38] used Schnyder woods to show that each 4-connected triangulation has a contact representation with homothetic triangles. Gonçalves et al. [30] extended the triangle-contact results from triangulations [23] to 3-connected plane graphs, by showing that Felsner's generalized Schnyder woods [25] correspond to *primal-dual* triangle-contact representations. Note that triangles and coins are not the only families of shapes that have been studied from the perspective of contact representations. Some further examples include boxes in $\mathbb{R}^3$ [18, 26, 41], line segments [22, 32], and homothetic polygons [20, 28, 37].

The construction of triangle-contact representations [23] (and the correspondence to 3-orientations) can be adjusted so that each triangle is the lower-right half of an axis-parallel rectangle. These *right-triangle representations (RT-representations)* are our focus; see Fig. 3.

Our Contribution and Outline. The paper is organized as follows. We start with some definitions in Section 2 and describe the relationship between (degenerate) RT-representations and Schnyder woods of plane triangulations in Section 3. In Section 4, we provide necessary and sufficient conditions for a linear morph between two RT-representations. The first condition is that each corner c of a triangle touches the same side s of another triangle in the two representations, that is, the morph happens within the same Schnyder wood. The contact between c and s is always maintained when s has the same slope in the two RT-representations. Otherwise, we require the point of s hosting c to be defined by the same convex combination of the end-points of s in both representations. In Section 5, we present our morphing algorithm. If the two input RT-representations correspond to different Schnyder woods, we consider a path between them in the lattice structure of all Schnyder woods, similar to [12], that satisfies some properties (if it exists). When moving along this path, from a Schnyder wood to another, we construct intermediate RT-representations that simultaneously correspond to both woods. We provide an algorithm to construct such intermediate RT-representations that result in a linear morph at each step. Finally, in Section 6, we show how to decide whether there is a path in the lattice structure that satisfies the required properties. This results in an efficient testing algorithm for the existence of a piecewise linear morph

(a) inner vertex **(b)** outer vertices

Figure 1 The two conditions for a Schnyder wood.

between two RT-representations of a plane triangulation; in the positive case, the computed piecewise linear morph has at most quadratic length. Consequently, for 4-connected plane triangulations, under a natural condition on the outer face of their RT-representations, the topological space defined by such RT-representations is connected.

2 Definitions and Preliminaries

Basics. A *plane triangulation* is a maximal planar graph with a distinguished outer face. A *directed acyclic graph (DAG)* is an oriented graph with no directed cycles. A *topological ordering* of an n-vertex DAG $G = (V, E)$ is a one-to-one map $\tau : V \to \{1, \ldots, n\}$ such that $\tau(v) < \tau(w)$ for $(v, w) \in E$. Let p and q be two points in the plane. The *line segment* $\overline{pq}$ is the set $\{(1 - \lambda)p + \lambda q;\ 0 \leq \lambda \leq 1\}$ of convex combinations of p and q. Considering $\overline{pq}$ *oriented* from p to q, we say that x *cuts* $\overline{pq}$ *with the ratio* λ if $x = (1 - \lambda)p + \lambda q$.

In the case of polygons, a linear morph is completely specified by the initial and final positions of the corners of each polygon. If a corner p is at position p_0 in the initial representation (at time $t = 0$) and at position p_1 in the final representation (at time $t = 1$), then its position at time t during a linear morph is $(1 - t)p_0 + tp_1$ for any $0 \leq t \leq 1$.

Schnyder Woods. A *3-orientation* [15, 25] of a plane triangulation is an orientation of the inner edges such that each inner vertex has out-degree 3 and the three outer vertices have out-degree 0. A *Schnyder wood* T [36] of a plane triangulation G is a 3-orientation together with a partition of the inner edges into three color classes, such that the three outgoing edges of an inner vertex have distinct colors and all the incoming edges of an outer vertex have the same color. Moreover, the color assignment around the vertices must be as indicated in Fig. 1. We say that a cycle in a Schnyder wood is *oriented* if it is a directed cycle.

The following well-known properties of Schnyder woods can directly be deduced from the work of Schnyder [36]. **1.** Every plane triangulation has a 3-orientation. **2.** For each 3-orientation of a plane triangulation there is exactly one partition of the inner edges into three color classes such that the pair yields a Schnyder wood. **3.** Each color class of a Schnyder wood induces a directed spanning tree rooted at an outer vertex. **4.** Reversing the edges of two color classes and maintaining the orientation of the third color class yields a directed acyclic graph. **5.** The edges of an oriented triangle in a Schnyder wood have three distinct colors and every triangle composed of edges of three different colors is oriented.

We call the color classes red (r,→), blue (b,→), and green (g,→). The symbols X_r, X_b, and X_g denote the *red*, *blue*, and *green outer vertex* of G, i.e., the outer vertices with incoming red, blue, and green edges, respectively. For an inner vertex v, let v_r, v_b, and v_g be the respective neighbors of v such that (v, v_r) is red, (v, v_b) is blue, and (v, v_g) is green. Finally, let $\mathrm{DAG}_r(T)$ ($\mathrm{DAG}_b(T)$) be the directed acyclic graph obtained from G by orienting all red (blue) edges as in T while all blue (red) and green edges are reversed.

Let C be an oriented triangle of a Schnyder wood T. Reversing C yields another 3-orientation with its unique Schnyder wood T_C. If C is a facial cycle, then T differs from T_C by recoloring the edges on C only. More precisely, the former outgoing edge of a vertex gets the color of the former incoming edge of the same vertex. This procedure of reversing and recoloring is called *flipping*[5] an oriented triangle of a Schnyder wood. Any Schnyder wood can be converted into any other Schnyder wood of the same plane triangulation by flipping $\mathcal{O}(n^2)$ oriented triangles [12, 15]. For two Schnyder woods T_0 and T_ℓ, $<C_1, \ldots, C_\ell>$ is a *flip sequence between* T_0 *and* T_ℓ if there are Schnyder woods $T_1, \ldots, T_{\ell-1}$ such that C_i, $i = 1, \ldots, \ell$, is an oriented triangle in T_{i-1} and T_i is obtained from T_{i-1} by flipping C_i. We say that *a Schnyder wood* T' *can be obtained from a Schnyder wood* T *by a sequence of facial flips* if there is a flip sequence between T and T' that contains only facial cycles.

3 RT-Representations of Plane Triangulations

Let R be an RT-representation of a plane triangulation G and let u be a vertex of G. Recall that $\Delta(u)$ is the triangle representing u in R. We denote by $\_(u)$, $|(u)$, and $/(u)$ the *horizontal*, *vertical*, and *diagonal* side of $\Delta(u)$. Further, we denote by $\angle(u)$, $\dashv(u)$, and $\wedge(u)$, the left, right, and top corner of $\Delta(u)$, respectively. If two triangles touch each other in their corners, we say that these two corners *coincide*. If there exist no two triangles whose corners coincide, then R is *non-degenerate*; otherwise, it is *degenerate*. Let (c, s) be a pair with $c \in \{\angle, \dashv, \wedge\}$ and $s \in \{|, \_, /\}$, we say that (c, s) is a *compatible pair* if it belongs to the set $\{(\dashv, /), (\angle, |), (\wedge, \_)\}$. Observe that, in any RT-representation of G, if a corner c of a triangle $\Delta(u)$ touches the side s of a triangle $\Delta(v)$, with $(u, v) \in E(G)$, then (c, s) is a compatible pair. We formally require this also in the case of a degeneracy. E.g., if $\dashv(v)$ coincides with $\angle(u)$ for two vertices u and v, then the respective compatible pair is either $(\angle, |)$ or $(\dashv, /)$ – even though $\dashv(v)$ also touches $\_(u)$, and $\angle(u)$ touches $\_(v)$.

In the next two subsections, we describe the relationship between RT-representations and Schnyder woods [23] and extend it to the case of degenerate RT-representations.

3.1 From RT-Representations to Schnyder Woods

Let $G = (V, E)$ be a plane triangulation with a given RT-representation R. It is possible to orient and color the edges of G in order to obtain a Schnyder wood by considering the types of contacts between triangles in R as follows.

First, consider the non-degenerate case; refer to Fig. 2a. Let $e = \{u, v\} \in E$ be an inner edge such that a corner c of $\Delta(u)$ touches a side s of $\Delta(v)$. We use the following rules: We orient e from u to v, and color e **blue** if c is $\angle(u)$, **green** if c is $\dashv(u)$, **red** if c is $\wedge(u)$.

▶ **Lemma 1** ([23], Theorem 2.2). *The above assignment yields a Schnyder wood.*

Assume now that there exist two triangles $\Delta(u)$ and $\Delta(v)$ whose corners coincide. Observe that the assignment of colors and directions to the edge $\{u, v\}$ determined by the procedure above would be ambiguous. The next observation will be useful to resolve this ambiguity.

▶ **Observation 2.** *In an RT-representation of a plane triangulation, if the corner of a triangle* $\Delta(u)$ *coincides with the corner of a triangle* $\Delta(v)$ *in a point* p*, then there exists a triangle* $\Delta(w)$*,* $w \neq u, v$*, with a corner on* p*, unless* $\{u, v\}$ *is an edge of the outer face.*

[5] Brehm [15] called flipping a counter clockwise triangle a flip, and flipping a clockwise triangle a flop.

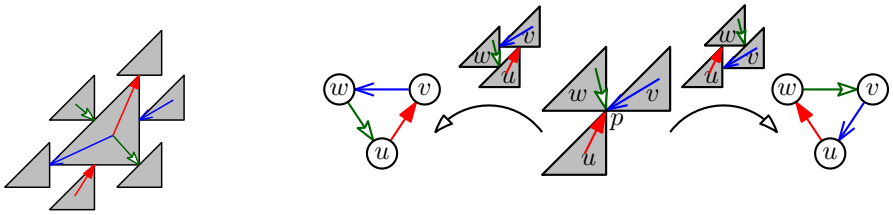

(a) non-degenerate case **(b)** degenerate case

Figure 2 From an RT-representation to a Schnyder wood.

By Observation 2, in a degenerate RT-representation there exist three vertices u, v, and w such that $\nearrow\!\!\sqcap(u)$, $\sqcup\!\!\angle(v)$, $\sqcup\!\!\perp(w)$ lie on a point, see Fig. 2b. For each of the three edges, a choice of coloring and orientation corresponds to deciding which of the two triangles participates to the touching with its corner and which triangle with an extremal point of one of its sides. This yields two options as indicated in Fig. 2b, both resulting in a Schnyder wood. Note that the face $f = \langle u, v, w\rangle$ is cyclic in both these Schnyder woods, and each of them can be obtained from the other by flipping f. Summarizing, we get the following.

▶ **Observation 3.** *Given an RT-representation R of a plane triangulation G, let P be the set of points where three triangles meet. Then, R corresponds to a set $\mathcal{T}_R$ of $2^{|P|}$ different Schnyder woods on G, the points of P correspond to $|P|$ edge-disjoint oriented triangles, and the Schnyder woods in $\mathcal{T}_R$ differ in flipping some of them.*

3.2 From Schnyder Woods to RT-Representations

Assume now that we are given a Schnyder wood T of a plane triangulation $G = (V, E)$. We describe a technique for constructing an RT-representation of G corresponding to T in which the y-coordinate of the horizontal side of each triangle is prescribed by a function $\tau : V \to \mathbb{R}$ satisfying some constraints; observe that in the non-degenerate case in [23] τ is a topological labeling of $\mathrm{DAG}_r(T)$, i.e., a canonical ordering of G.

We call $\tau : V \longrightarrow \mathbb{R}$ an *Admissible Degenerate Topological* labeling of the graph $\mathrm{DAG}_r(T)$, for short *ADT-labeling*, if for each directed edge (u, v) of $\mathrm{DAG}_r(T)$, we have **1.** $\tau(u) \leq \tau(v)$ and **2.** $\tau(u) = \tau(v)$ only if **a.** is green and belongs to a clockwise oriented facial cycle, or **b.** is blue and belongs to a counter-clockwise oriented facial cycle, and **3.** if $\tau(u_b) = \tau(u) = \tau(u_g)$ for a vertex u, and u_1 and u_2 are vertices such that $\langle u, u_g, u_1\rangle$ is a clockwise facial cycle and $\langle u, u_b, u_2\rangle$ is a counter-clockwise facial cycle, then $u_1 \neq u_2$.

▶ **Lemma 4.** *Let R be an RT-representation of a plane triangulation $G = (V, E)$, let T be a Schnyder wood corresponding to R, and let $\tau(v)$, $v \in V$, be the y-coordinate of $\llcorner(v)$. Then, τ is an ADT-labeling of $\mathrm{DAG}_r(T)$.*

Proof. Let (u, v) be a directed edge of $\mathrm{DAG}_r(T)$. By the definition of T, we get immediately that $\tau(u) \leq \tau(v)$ independently of whether (u, v) is red, green, or blue. In fact, if (u, v) is red, then it is oriented from u to v in T_r. Thus, the compatible pair corresponding to such an edge in R is $(\nearrow\!\!\sqcap(u), \llcorner(v))$. Hence, $\llcorner(u)$ lies strictly below $\llcorner(v)$. If (u, v) is green (resp., blue), then it is oriented from v to u in T. Thus, the compatible pair corresponding to such an edge in R is $(\sqcup\!\!\perp(v), \nearrow(u))$ (resp., $(\sqcup\!\!\angle(v), \nwarrow(u))$). Hence, $\llcorner(u)$ does not lie above $\llcorner(v)$.

Assume that $\tau(u) = \tau(v)$, which implies that (u, v) is not red, as observed above. Suppose that (v, u) is a green edge. Then, $\sqcup\!\!\perp(v)$ and $\sqcup\!\!\angle(u)$ coincide. By Observation 2, there exists a vertex z such that $\nearrow\!\!\sqcap(z)$ coincides with $\sqcup\!\!\perp(v)$ and $\sqcup\!\!\angle(u)$. Thus, $\langle v, u, z\rangle$ is a clockwise

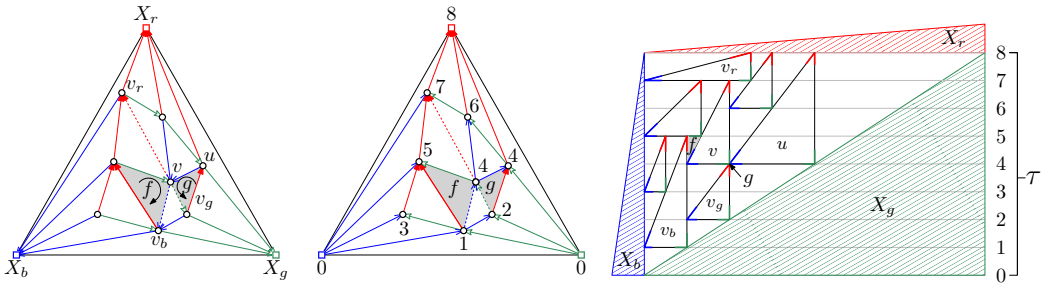

(a) Schnyder wood of G **(b)** Labeling τ of G **(c)** RT(T, τ, R_o)

Figure 3 (a) A Schnyder wood T of a plane triangulation G; the edges connecting v with vertices v_r, v_g, and v_b are dashed. (b) Graph DAG$_r(T)$ with ADT-labeling τ. (c) An RT-representation of G constructed from T, τ, and an RT-representation R_o of the outer face.

oriented facial cycle. Similarly, when (v, u) is a blue edge, there is a vertex z such that $\angle(v)$, $\angle(u)$, and $\angle(z)$ coincide. Therefore, $\langle v, u, z\rangle$ is a counter-clockwise oriented facial cycle.

Finally, if $\tau(u_b) = \tau(u) = \tau(u_g)$ and u_1 and u_2 are the vertices such that $\langle u, u_g, u_1\rangle$ is a clockwise facial cycle and $\langle u, u_b, u_2\rangle$ is a counter-clockwise facial cycle, then $\angle(u_1)$ touches $\angle(u)$ and $\angle(u_2)$ touches $\angle(u)$. Thus, $u_1 \neq u_2$. ◀

▶ **Lemma 5.** *Let T be a Schnyder wood of an n-vertex plane triangulation G, let τ be an ADT-labeling of* DAG$_r(T)$*, and let $R_o = \Delta(X_r) \cup \Delta(X_g) \cup \Delta(X_b)$ be an RT-representation of the outer face of G such that $\angle(X_i)$ has y-coordinate $\tau(X_i)$, with $i \in \{r, g, b\}$. Then, there exists a unique RT-representation* RT(T, τ, R_o) *of G corresponding to T in which $\angle(v)$ has y-coordinate $\tau(v)$, for each vertex v of G, and in which the outer face is drawn as in R_o.*

Outline of the Proof. We process the vertices of G according to a topological ordering τ' of DAG$_r(T)$. In the first two steps, we draw triangles $\Delta(X_b)$ and $\Delta(X_g)$ as in R_o; see Fig. 3c. At each of the following steps, we consider a vertex v, with $2 < \tau'(v) = i < n$.

We draw $\Delta(v)$ with its horizontal side on $y = \tau(v)$ and with its top corner at $y = \tau(v_r)$, as follows. Since the blue edge (v_b, v) and the green edge (v_g, v) are entering v in DAG$_r(T)$, the triangles $\Delta(v_b)$ and $\Delta(v_g)$ have already been drawn. Also, by Property 1 of ADT-labeling, we have that $\tau(v_b) \leq \tau(v)$ and $\tau(v_g) \leq \tau(v)$. Further, it can be shown that $\angle(v_b)$ and $\angle(v_g)$ have y-coordinate larger than or equal to $\tau(v)$, and that if a triangle $\Delta(u)$ intersects the line $y = \tau(v)$ between $\Delta(v_b)$ and $\Delta(v_g)$, then u is a neighbor of v such that $v = u_r$. By construction, $\angle(u)$ has y-coordinate equal to $\tau(v)$. Thus, we draw the horizontal side of $\Delta(v)$ on $y = \tau(v)$ between $\Delta(v_b)$ and $\Delta(v_g)$. The conditions of ADT-labelings guarantee that $\angle(v)$ has positive length. If $i = n$, and hence $v = X_r$, we draw $\Delta(X_r)$ as in R_o. ◀

4 Geometric Tools

In this section, we provide geometric lemmata that will be exploited in the subsequent sections. We first show that the incidence of a point and a line segment is maintained during a linear morph if the line segment is moved in parallel (with a possible stretch, but keeping the orientation) or the ratio with which the point cuts the segment is maintained; see Fig. 4.

▶ **Lemma 6.** *For $i = 0, 1$ let p_i, q_i be two points in the plane and let $x_i \in \overline{p_i q_i}$. For $0 < t < 1$, further let $p_t = (1-t)p_0 + tp_1$ and $q_t = (1-t)q_0 + tq_1$. Then, $x_t = (1-t)x_0 + tx_1 \in \overline{p_t q_t}$ if*

1. *$\overline{p_0 q_0}$ and $\overline{p_1 q_1}$ are parallel with the same direction, or*
2. *x_0 cuts $\overline{p_0 q_0}$ with the same ratio as x_1 cuts $\overline{p_1 q_1}$*

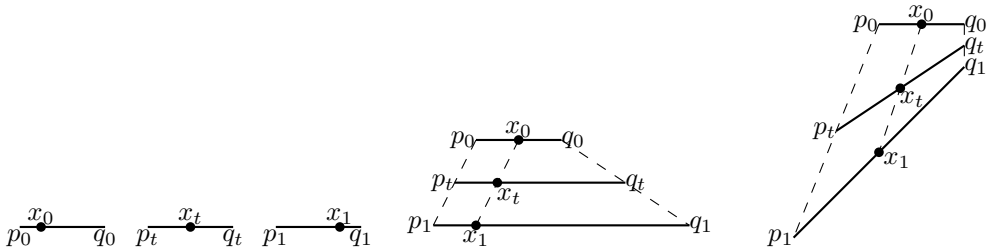

(a) segments collinear **(b)** segments parallel **(c)** cut ratio maintained

Figure 4 Morphing a segment and a point.

Proof. Assume first that $\overline{p_0q_0}$ and $\overline{p_1q_1}$ are parallel. If $\overline{p_0q_0}$ and $\overline{p_1q_1}$ are collinear, we may assume that they are both contained in the x-axis, that p_i, q_i, $i = 0, 1$, are real numbers, and that $p_0 < q_0$. Since $\overline{p_0q_0}$ and $\overline{p_1q_1}$ have the same direction, this implies that $p_1 < q_1$. Since x_i, $i = 0, 1$, is a point in $\overline{p_iq_i}$, it follows that $p_i \leq x_i \leq q_i$. Hence, we get for $t \in [0, 1]$ that

$$\underbrace{(1-t)p_0 + tp_1}_{p_t} \leq \underbrace{(1-t)x_0 + tx_1}_{x_t} \leq \underbrace{(1-t)q_0 + tq_1}_{q_t}.$$

If $\overline{p_0q_0}$ and $\overline{p_1q_1}$ are parallel with the same direction but not collinear, then the polygon $\langle p_0, q_0, q_1, p_1\rangle$ is convex. Thus, $\overline{x_0x_1}$ must intersect $\overline{p_tq_t}$, for any t. Also, $\overline{p_tq_t}$ and x_t both lie on the same line ℓ_t. More precisely, let d be the distance between the lines through segments $\overline{p_0q_0}$ and $\overline{p_1q_1}$. Then, ℓ_t is the line with distance td from $\overline{p_0q_0}$.

Finally, if x_0 cuts $\overline{p_0q_0}$ with the same ratio λ as x_1 cuts $\overline{p_1q_1}$, then $x_t = (1-t)((1-\lambda)p_0 + \lambda q_0) + t((1-\lambda)p_1 + \lambda q_1) = (1-\lambda)p_t + \lambda q_t \in \overline{p_tq_t}$. ◀

Lemma 6 implies the following sufficient criterion for a linear morph.

▶ **Lemma 7.** *Let R_0 and R_1 be two RT-representations of a triangulation G corresponding to the same Schnyder wood such that the triangles of the outer face pairwise touch in their corners. The pair $\langle R_0, R_1\rangle$ defines a linear morph if, for any two adjacent vertices u and v such that a corner $c_i(v)$ of v touches a side $s_i(u)$ of u, where $c \in \{$ ◪, ◿, ◪ $\}$ and $s \in \{$ ◿, ◪, ◿ $\}$, one of the following holds:*
1. *$s_1(u)$ and $s_2(u)$ are parallel.* ***2.*** *$c_1(v)$ cuts $s_1(u)$ with the same ratio as $c_2(v)$ cuts $s_2(u)$.*

By Observation 3, an RT-representation R of a plane triangulation G corresponds to a set $\mathcal{T}_R$ of Schnyder woods that differ from each other by flipping a set of edge disjoint triangles. The *topmost* vertex of R is the vertex v of G maximizing the y-coordinate of ◿(v).

▶ **Lemma 8.** *Let R_0 and R_1 be two RT-representations of the same plane triangulation $G = (V, E)$ such that $\langle R_0, R_1\rangle$ is a linear morph. Then $\mathcal{T}_{R_0} \cap \mathcal{T}_{R_1} \neq \emptyset$.*

▶ **Theorem 9** (Necessary Condition)**.** *If there is a piecewise linear morph between two RT-representations of a plane triangulation G, then the corresponding Schnyder woods can be obtained from each other by a sequence of facial flips. In particular the topmost vertex is the same in both representations if G has more than three vertices.*

Proof. Let $\langle R_1, \ldots, R_\ell\rangle$ be a sequence of linear morphs. Lemma 8 implies $\mathcal{T}_{R_i} \cap \mathcal{T}_{R_{i+1}} \neq \emptyset$ for $i = 1, \ldots, \ell - 1$. Let $T_i \in \mathcal{T}_{R_i} \cap \mathcal{T}_{R_{i+1}}$ for $i = 1, \ldots, \ell - 1$. Then T_{i+1}, $i = 1, \ldots, \ell - 2$ can be obtained from T_i by a sequence of edge-disjoint facial flips. Hence, the Schnyder wood $T_{\ell-1}$ of R_ℓ can be obtained from the Schnyder wood T_1 of R_1 by a sequence of facial flips. ◀

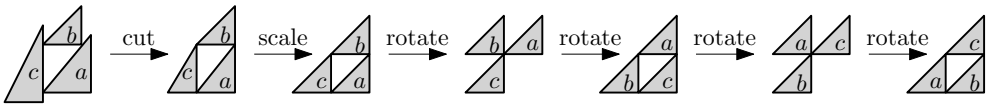

Figure 5 Morphing an RT-representation of a triangle to a labeled canonical form: First, cut the extruding parts of the triangles, maintaining the slopes of the diagonal sides. Then, scale the triangles such that the horizontal and vertical sides have length one. Finally, keep rotating the triangles until the topmost vertex is as desired.

5 A Morphing Algorithm

In this section, we prove the following theorem.

▶ **Theorem 10** (Sufficient Condition). *Let R_1 and R_2 be two RT-representations of an n-vertex plane triangulation G corresponding to the Schnyder woods T_1 and T_2, respectively. If T_2 can be obtained from T_1 by a sequence of ℓ facial flips, then there exists a piecewise linear morph between R_1 and R_2 of length $\mathcal{O}(n+\ell)$. Such a morph can be computed in $\mathcal{O}(n(n+\ell))$ time, provided that the respective sequence of ℓ facial flips is given.*

Since there is always a piecewise linear morph between two RT-representations of a plane triangle (see Fig. 5), we will assume that G has at least four vertices. This implies especially that the topmost vertex, which always coincides with X_r, is the same in R_1 and R_2.

In Section 5.1, we introduce our main procedure ADJUST, which moves a triangle in an RT-representation along an incident diagonal and adjusts the remaining triangles so that the result is a linear morph. Repeatedly applying ADJUST, we first morph R_1 to a non-degenerate RT-representation that still corresponds to T_1 (Section 5.3); then, we perform a sequence of linear morphs to realize the ℓ facial flips geometrically (Section 5.2), hence obtaining an RT-representation corresponding to T_2, which we finally morph to R_2 (Section 5.3).

5.1 Moving a Triangle Along a Diagonal

Let $G = (V, E)$ be a plane triangulation and let R be an RT-representation of G corresponding to a Schnyder wood T of G. Given an inner vertex x of G and a real value y with some properties, ADJUST computes a new RT-representation R' of G corresponding to T in which $\llcorner(x)$ has y-coordinate y and $\Delta(x_g)$ remains unchanged, such that $\langle R, R' \rangle$ is a linear morph.

To achieve this goal, the y-coordinate of $\llcorner(v)$, for some vertex $v \neq x$, may also change; however, the ratio with which $\llcorner(v)$ cuts $\llcorner(v_g)$ does not change, thus satisfying Property 2 of Lemma 7. The y-coordinates of the horizontal sides are encoded by a new ADT-labeling τ of G, and R' is the unique RT-representation $\mathrm{RT}(T, \tau, R_o)$ of G that is obtained by applying Lemma 5 with input G, T, τ, and the representation R_o of the outer face of G in R.

For a vertex $w \in V$, we denote by $\mathrm{top}(w)$ the y-coordinate of $\top(w)$; recall that, in our construction, we have $\mathrm{top}(w) = \tau(w_r)$, if w is an inner vertex. Also, let $v_1, \ldots, v_\ell$ be the neighbors of w such that $\llcorner(v_1), \ldots, \llcorner(v_\ell)$ appear in this order from $\angle(w)$ to $\top(w)$ along $\llcorner(w)$. For a fixed $i \in \{1, \ldots, \ell\}$, we say that *moving v_i to $y \in \mathbb{R}$ respects the order along $\llcorner(w)$* if (i) $i = 1$ and $\tau(w) \leq y < \tau(v_2)$ (where equality is only allowed if $\angle(v_1)$ does not lie on $\lrcorner(w_b)$), (ii) $i = 2, \ldots, \ell - 1$ and $\tau(v_{i-1}) < y < \tau(v_{i+1})$, or (iii) $i = \ell$ and $\tau(v_{i-1}) < y \leq \mathrm{top}(w)$ and $y < \mathrm{top}(v_\ell)$. Further, for a vertex v, we consider the ratio $\lambda(v)$ with which $\llcorner(v)$ cuts the incident diagonal side, i.e., $\lambda(v) = \frac{\tau(v) - \tau(v_g)}{\mathrm{top}(v_g) - \tau(v_g)}$, if either v is an inner vertex or $v \in \{X_b, X_r\}$, $\llcorner(v)$ is on $\llcorner(X_g)$, and $v_g := X_g$.

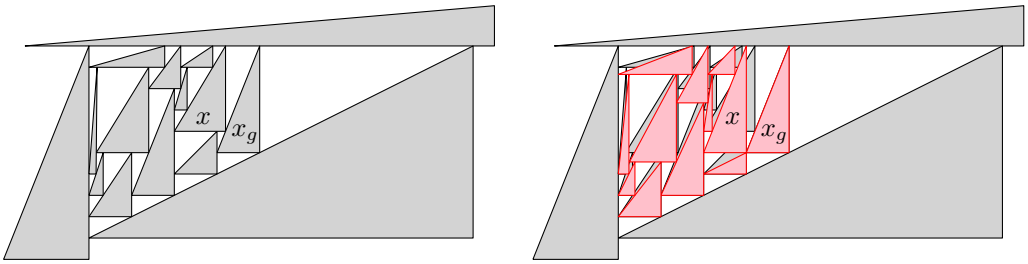

(a) original RT-representation **(b)** after applying ADJUST$(.,.,x,\tau(x_g))$.

Figure 6 Moving $\Delta(x)$ down along $\swarrow(x_g)$.

For the vertex x and the y-coordinate y that are part of the input of ADJUST, we assume that moving x to y respects the order along $\swarrow(x_g)$. Setting $\tau(x) \leftarrow y$ may have implications on the neighbors of x of the following type. **A.** For every vertex v such that $x = v_g$, the value of $\tau(v)$ has to be modified to ensure that the ratio $\lambda(v)$ with which $\perp(v)$ cuts $\swarrow(x)$ is maintained; **B.** for every vertex u such that $x = u_r$, we have to set $\text{top}(u) = y$ to maintain the contact between $\Delta(u)$ and $\Delta(x)$. Since these modifications may change the diagonal side of $\Delta(u)$ and $\Delta(v)$, they may trigger analogous implications for the neighbors of u and v.

Since the y-coordinate of $\perp(u)$ is not changed, only a type-A implication may be triggered for the neighbors of u. Further, the two implications correspond to following either a red or a green edge, respectively, in reverse direction with respect to the one in T. Hence, the vertices whose triangles may need to be adjusted are those that can be reached from the vertex x by a reversed directed path in T using only red and green edges, but no two consecutive red edges; see Fig. 7. Note that, since the green and the red edges have opposite orientation in T and in $\text{DAG}_b(T)$, which is acyclic, this implies that ADJUST terminates.

The procedure ADJUST (see Fig. 6 for an illustration) first finds all the triangles that may need to be adjusted, by performing a simple graph search from x following the above described paths of red and green edges. In a second pass, it performs the adjustment of each triangle $\Delta(w)$, by modifying $\tau(w)$ so that $\lambda(w)$ is maintained. We ensure that the new value of $\tau(w)$ is computed only after the triangle $\Delta(w_g)$ has already been adjusted.

▶ **Lemma 11.** *Let R_1 be an RT-representation of a plane triangulation $G = (V, E)$ corresponding to the Schnyder wood T and let the y-coordinate of $\perp_1(v)$ be $\tau_1(v)$, $v \in V$. Let $x \in V$ be an inner vertex and let $y \in \mathbb{R}$ be such that moving x to y respects the order along $\swarrow(x_g)$. Let τ_2 be the output of ADJUST(τ_1, T, x, y).*

Then, we have that (i) $\tau_2(x) = y$, (ii) $\lambda(v)$ is maintained for any vertex $v \neq x$, (iii) τ_2 is an ADT-labeling of $DAG_r(T)$, and (iv) the morph between R_1 and $R_2 = \text{RT}(T, \tau_2, R_o)$ is linear, where $R_o = \Delta_1(X_b) \cup \Delta_1(X_g) \cup \Delta_1(X_r)$.

Outline of the Proof. Properties i and ii are clear from the construction. We establish a cycle C' (see Fig. 7) that encloses all vertices for which τ might be changed. Distinguishing the cases $y < \tau_1(x)$ and $y > \tau_1(x)$, Properties iii can be shown by induction on a suitable ordering of the edges in $\text{DAG}_r(T)$. Since all predecessors of x_g in $\text{DAG}_b(T)$ are outside or on C', we have that $\Delta_1(x_g) = \Delta_2(x_g)$. Now, by Lemma 7, $\langle R_1, R_2 \rangle$ is a linear morph. ◀

5.2 A Flipping Algorithm

Recall that, given a Schnyder wood T and an oriented cycle C in T, the Schnyder wood T_C is obtained from T by flipping C. In the following theorem we show how to realize this flip geometrically with two linear morphs in the case in which C is a facial cycle.

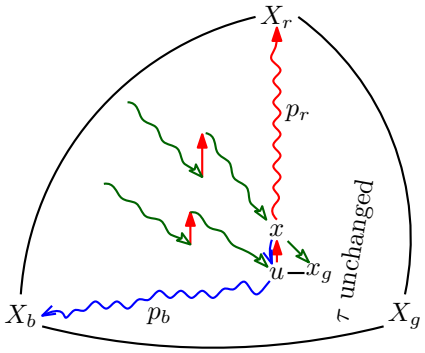

Figure 7 Let u be the neighbor of x following x_g in clockwise order. Then, the cycle C' composed of the blue u-X_b-path p_b, the edge $\{u, x\}$, the red x-X_r-path p_r, and the edge $\{X_r, X_b\}$ encloses all vertices for which τ is changed. Vertex x is the only vertex on C' for which τ is changed.

▶ **Theorem 12.** *Let R_1 be a non-degenerate RT-representation of a plane triangulation G corresponding to a Schnyder wood T. Let C be an oriented facial cycle in T. We can construct a sequence of two linear morphs $\langle R_1, R_2, R_3\rangle$ such that R_3 is a non-degenerate RT-representation of G corresponding to a Schnyder wood T_C.*

Proof. For the oriented facial cycle C, let C_r, C_g, and C_b be the vertices with outgoing red, green, and blue edge, respectively, in C. In order to flip C, we move C_g along the respective incident diagonal sides as sketched in the following figure.

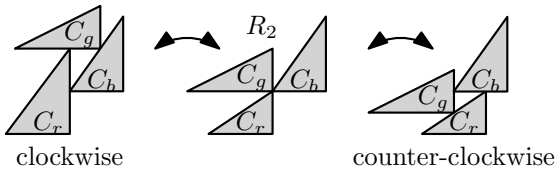

More precisely, let τ_1 be the y-coordinates of the horizontal sides in R_1. We first compute $\tau_2 \leftarrow \text{ADJUST}(\tau_1, T, C_g, \tau_1(C_b))$. If C is clockwise oriented, we then compute

$$\tau_3 \leftarrow \text{ADJUST}(\tau_2, T_C, C_g, (\tau_2(C_g) + \max\{\tau_2(u);\ u = C_r \text{ or } u_g = C_r\})/2).$$

If C is counter-clockwise oriented, we proceed as follows.

$$\tau_3 \leftarrow \text{ADJUST}(\tau_2, T_C, C_g, (\tau_2(C_g) + \min\{\tau_2(u);\ u = (C_b)_r \text{ or } u_g = C_b\})/2).$$

In each case the new y-coordinates y for C_g are chosen such that moving C_g to y respects the order along the respective incident diagonal. Thus, ADJUST can be applied. Also, τ_2 is an ADT-labeling of both, $\text{DAG}_r(T)$ and $\text{DAG}_r(T_C)$, and τ_3 is an ADT-labeling of $\text{DAG}_r(T_C)$. Let $R_2 = \text{RT}(T, \tau_2, R_o) = \text{RT}(T_C, \tau_2, R_o)$ and let $R_3 = \text{RT}(T_C, \tau_3, R_o)$. Since τ_2 and τ_3 are produced by ADJUST, by Lemma 11, both $\langle R_1, R_2\rangle$ and $\langle R_2, R_3\rangle$ are linear morphs. ◀

5.3 Morphing Representations with the same Schnyder Wood

In this section, we consider RT-representations corresponding to the same Schnyder Wood.

▶ **Theorem 13.** *Let R_1 and R_2 be two RT-representations of an n-vertex plane triangulation corresponding to the same Schnyder wood T. Then, there is a piecewise linear morph between R_1 and R_2 of length at most $2n$.*

The idea is to first transform the outer face to a canonical form, and then to move one vertex v per step to a new y-coordinate y such that the ratio $\lambda(v)$ is set to how it should be in R_2. The order in which we process the vertices is such that ADJUST can be applied to the vertex v and the y-coordinate y. Recall that ADJUST does not alter the ratio λ, except for the currently processed vertex v. The following lemma can be proven by induction on n.

▶ **Lemma 14.** *Let $P = \{p_1 < \cdots < p_n\}$ and $Q = \{q_1 < \cdots < q_n\}$ be two sets of n reals each. If $P \neq Q$ then there is an i such that $p_i \neq q_i$ and P has no element between p_i and q_i.*

▶ **Corollary 15.** *Let P and Q each be a set of n points on a segment s. We can move P to Q in n steps by moving one point per step and by maintaining the ordering of the points on s.*

Proof of Theorem 13. Let τ' be a topological ordering of the inner vertices of $\mathrm{DAG}_r(T)$. We extend τ' to an ADT-labeling of $\mathrm{DAG}_r(T)$ by setting $\tau'(X_b) = 0 = \tau'(X_g)$, and $\tau'(X_r) = n-2$. With a sequence of at most n linear morphs we transform R_i, $i = 1, 2$, into an RT-representation $R' = \mathrm{RT}(T, \tau', R_o)$, where R_o has the following *canonical form*: $\llcorner(X_b) = \angle(X_g) = (0,0)$, $\nwarrow(X_b) = \angle(X_r) = (0, n-2)$, $\nwarrow(X_g) = \llcorner(X_r) = (n-2, n-2)$, and the lengths of $\blacktriangleleft(X_r)$ and $\blacktriangle(X_b)$ are one. In the first morph, we cut the extruding parts of the outer triangles. In the second morph, we independently scale the x- and y-coordinates of the corners and translate the drawing, to fit the corners as indicated. In a third step, we adjust the lengths of $\blacktriangleleft(X_r)$ and $\blacktriangle(X_b)$. In the first morph the slope of no side is changed, in the second morph no ratio is changed, and in the third morph there are only four sides that are changed, which are not incident to any other triangle. Thus, the three morphs are linear. Let the resulting RT-representation be R'_i.

We now process the vertices in a reversed topological ordering on $\mathrm{DAG}_b(T)$. We process a vertex w as follows. Let τ be the current y-coordinates of the horizontal sides. Let $\mathcal{G}(w) = \{v \in V; w = v_g\}$ and let $P = \{\tau(v);\ v \in \mathcal{G}(w)\}$. For $v \in \mathcal{G}(w)$ let $y(v)$ be such that

$$\frac{y(v) - \tau(w)}{\tau(w_r) - \tau(w)} = \frac{\tau'(v) - \tau'(w)}{\tau'(w_r) - \tau'(w)},$$

i.e., placing $\blacktriangle(v)$, $v \in \mathcal{G}(w)$ on the y-coordinate $y(v)$ cuts $\blacktriangleright(w)$ in the the same ratio as in R'. Let $Q = \{y(v);\ v \in \mathcal{G}(w)\}$. By the above corollary, we can order $\mathcal{G}(w) = \{v_1, \ldots, v_k\}$ such that replacing in the i*th* step $\tau(v_i)$ by $y(v_i)$ maintains the ordering of $\{\tau(v);\ v \in \mathcal{G}(w)\}$. Since τ' is a topological ordering, we will not move $\llcorner(v_i)$ to an end vertex of $\blacktriangleright(w)$. For $i = 1, \ldots, k$ we now call $\tau \leftarrow \textsc{adjust}(\tau, T, v_i, y(v_i))$. This yields one linear morphing step.

After processing all vertices w in a reversed topological ordering of $\mathrm{DAG}_b(T)$ and all vertices in $\mathcal{G}(w)$ in the order given above, we have obtained an RT-representation R in which any right corner cuts its incident diagonal in the same ratio as in R'. Since the outer face is fixed, this implies that $R = R'$. Observe that $\mathcal{G}(w)$, $w \in V$, is a partition of the set of inner vertices. Hence, we get at most one morphing step for each of the $n-3$ inner vertices. ◀

Combining the results of Sections 5.1 to 5.3 yields the main result of the section.

Proof of Theorem 10. First, we transform R_1 into a non-degenerate RT-representation R with Schnyder wood T_1 and a canonical representation of the outer face in $\mathcal{O}(n)$ linear morphing steps, by Theorem 13. Then, we perform the ℓ facial flips as described in the proof of Theorem 12, using two linear morphs for each flip. This yields an RT-representation R' with Schnyder wood T_2. Finally, we transform R' into R_2 in $\mathcal{O}(n)$ linear morphing steps, by Theorem 13. This yields a total of $\mathcal{O}(n + \ell)$ linear morphs. Each linear morph can be computed by one application of ADJUST, which runs in linear time. ◀

6 A Decision Algorithm

It follows from Theorem 9 and Theorem 10 that there is a piecewise linear morph between two RT-representations of a plane triangulation if and only if the respective Schnyder woods can be obtained from each other by flipping faces only. Note that this condition is always satisfied if the triangulation is 4-connected and the topmost vertex is the same in both RT-representations. On the other hand, if the graph contains separating triangles, we have to decide whether there is such a sequence of facial flips. We will show that this can be decided efficiently and that, in the positive case, there exists one sequence whose length is at most quadratic in the number of vertices. This establishes our final result.

▶ **Theorem 16.** *Let R_1 and R_2 be two RT-representations of an n-vertex plane triangulation. We can decide in $\mathcal{O}(n^2)$ time whether there is a piecewise linear morph between R_1 and R_2 and, if so, a morph with $\mathcal{O}(n^2)$ linear morphing steps can be computed in $\mathcal{O}(n^3)$ time.*

Since there is a one-to-one correspondence between Schnyder woods of a plane triangulation and its 3-orientations, we will omit the colors in the following. A careful reading of Brehm [15] and Felsner [25] reveals the subsequent properties of 3-orientations. The set of 3-orientations of a triangulation forms a distributive lattice with respect to the following ordering. $T_1 \leq T_2$ if and only if T_1 can be obtained from T_2 by a sequence of flips on some counter-clockwise triangles. The minimum element is the unique 3-orientation without counter-clockwise cycles. Moreover, given a 3-orientation T and a triangle t, the number of occurrences of t in any flip-sequence between T and the minimum 3-orientation is the same – provided that the flip sequence contains only counter-clockwise triangles. Let this number be the potential $\pi_T(t)$.

Observe that π_T is distinct for distinct T. Moreover, $\min(\pi_{T_1}(t), \pi_{T_2}(t))$, t triangle, is the potential of the *meet* $T_1 \wedge T_2$ (i.e., the infimum) of two 3-orientations T_1 and T_2, while $\max(\pi_{T_1}(t), \pi_{T_2}(t))$, t triangle, is the potential of the *join* $T_1 \vee T_2$ (i.e., the supremum) of T_1 and T_2. The potential π_T can be computed in quadratic time for a fixed 3-orientation T of an n-vertex triangulation: At most $\mathcal{O}(n^2)$ flips have to be performed in order to reach the minimum 3-orientation. With a linear-time preprocessing, we can store all initial counter-clockwise triangles in a list. After each flip, the list can be updated in constant time.

▶ **Lemma 17.** *Let T_1 and T_2 be two 3-orientations of an n-vertex triangulation. T_1 can be obtained from T_2 by a sequence of facial flips if and only if $\pi_{T_1}(t) - \pi_{T_2}(t) = 0$ for all separating triangles t. Moreover, if T_1 can be obtained from T_2 by a sequence of facial flips, then it can be obtained by $\mathcal{O}(n^2)$ facial flips.*

Proof. Observe that going from T_1 to the meet $T_1 \wedge T_2$ involves

$$\pi_{T_1}(t) - \min(\pi_{T_1}(t), \pi_{T_2}(t)) \in \{0, \pi_{T_1}(t) - \pi_{T_2}(t)\}$$

counter-clockwise flips on triangle t, and going from the meet $T_1 \wedge T_2$ to T_2 involves

$$\pi_{T_2}(t) - \min(\pi_{T_1}(t), \pi_{T_2}(t)) \in \{0, \pi_{T_2}(t) - \pi_{T_1}(t)\}$$

clockwise flips on triangle t. Thus, if $\pi_{T_1}(t) - \pi_{T_2}(t) = 0$ for all separating triangles t, then no flip must be performed on a separating triangle. Then, the total number of flips is bounded by $\sum_{t \text{ face}} (\pi_{T_1}(t) + \pi_{T_2}(t)) \in \mathcal{O}(n^2)$.

Assume now that there is a sequence $T_1 = T'_0, T'_1, \ldots, T'_\ell, T'_{\ell+1} = T_2$ of 3-orientations such that T'_{i+1}, $i = 0, \ldots, \ell$, is obtained from T'_i by a (clockwise or counter-clockwise) facial flip. We show by induction on ℓ that $\pi_{T_1}(t) - \pi_{T_2}(t) = 0$ for all separating triangles t. If $\ell = 0$, let

t_0 be the triangle that has to be flipped in order to go from T_1 to T_2. Then, t_0 is a face and $\pi_{T_1}(t) - \pi_{T_2}(t) = 0$ for $t \neq t_0$. Assume now that $\ell \geq 1$. Let t be a separating triangle. Then

$$\pi_{T_1}(t) - \pi_{T_2}(t) = \underbrace{\pi_{T_1}(t) - \pi_{T'_\ell}(t)}_{=0 \text{ by IH}} + \underbrace{\pi_{T'_\ell}(t) - \pi_{T_2}(t)}_{=0 \text{ by IH}} = 0.$$ ◀

7 Conclusions and Open Problems

We have studied piecewise linear morphs between RT-representations of plane triangulations, and shown that when such a morph exists, there is one of length $\mathcal{O}(n^2)$. It would be interesting to explore lower bounds on this length. Observe that the minimum length of a flip-sequence containing only facial cycles does not immediately imply such bound, since some flips could be parallelized. Additionally, bounds on the resolution throughout our morphs would be worth investigating; however, it is unclear whether the "ratio fixing" we use would allow nice bounds. For this, it may help to return to integer y-coordinates between any two flips; however, this would result in a cubic number of linear morphing steps. A major open direction is whether our results can be lifted to general plane graphs, e.g., through the use of compatible triangulations. Note that such a compatible triangulation would need to be formed while preserving the conditions for the existence of a linear morph, i.e., without introducing the need to flip a separating triangle.

Finally, beyond the context of RT-representations, many other families of geometric objects could be considered. For example, morphing degenerate contact representations of line segments generalizes planar morphing, by treating contact points as vertices.

References

1 Soroush Alamdari, Patrizio Angelini, Fidel Barrera-Cruz, Timothy M. Chan, Giordano Da Lozzo, Giuseppe Di Battista, Fabrizio Frati, Penny Haxell, Anna Lubiw, Maurizio Patrignani, Vincenzo Roselli, Sahil Singla, and Bryan T. Wilkinson. How to Morph Planar Graph Drawings. *SIAM Journal on Computing*, 46(2):824–852, 2017.

2 Soroush Alamdari, Patrizio Angelini, Timothy M. Chan, Giuseppe Di Battista, Fabrizio Frati, Anna Lubiw, Maurizio Patrignani, Vincenzo Roselli, Sahil Singla, and Bryan T. Wilkinson. Morphing Planar Graph Drawings with a Polynomial Number of Steps. In Sanjeev Khanna, editor, *Proceedings of the 24th Annual ACM-SIAM Symposium on Discrete Algorithms, (SODA 2013)*, pages 1656–1667. SIAM, 2013.

3 Helmut Alt and Leonidas J. Guibas. Chapter 3 - Discrete Geometric Shapes: Matching, Interpolation, and Approximation. In J.-R. Sack and J. Urrutia, editors, *Handbook of Computational Geometry*, pages 121–153. North-Holland, Amsterdam, 2000.

4 E. M. Andreev. On convex polyhedra in Lobachevskij spaces. *Math. USSR, Sb.*, 10:413–440, 1971.

5 Patrizio Angelini, Steven Chaplick, Sabine Cornelsen, Giordano Da Lozzo, and Vincenzo Roselli. Morphing Contact Representations of Graphs. *CoRR*, abs/1903.07595, 2019. `arXiv:1903.07595`.

6 Patrizio Angelini, Giordano Da Lozzo, Giuseppe Di Battista, Fabrizio Frati, Maurizio Patrignani, and Vincenzo Roselli. Morphing Planar Graph Drawings Optimally. In Javier Esparza, Pierre Fraigniaud, Thore Husfeldt, and Elias Koutsoupias, editors, *Proceedings of the 41st International Colloquium on Automata, Languages, and Programming - 41st International Colloquium (ICALP 2014)*, volume 8572 of *LNCS*, pages 126–137. Springer, 2014.

7 Patrizio Angelini, Giordano Da Lozzo, Fabrizio Frati, Anna Lubiw, Maurizio Patrignani, and Vincenzo Roselli. Optimal Morphs of Convex Drawings. In Lars Arge and János Pach, editors,

Proceedings of the 31st International Symposium on Computational Geometry (SoCG 2015), volume 34 of *LIPIcs*, pages 126–140. Schloss Dagstuhl - Leibniz-Zentrum für Informatik, 2015.

8 Patrizio Angelini, Fabrizio Frati, Maurizio Patrignani, and Vincenzo Roselli. Morphing Planar Graph Drawings Efficiently. In Stephen K. Wismath and Alexander Wolff, editors, *Proceedings of the 21st International Symposium on Graph Drawing (GD 2013)*, volume 8242 of *LNCS*, pages 49–60. Springer, 2013.

9 Douglas N. Arnold and Jonathan Rogness. Möbius Transformations Revealed. *Notices of the AMS*, 55(10), 2008.

10 Boris Aronov, Raimund Seidel, and Diane Souvaine. On compatible triangulations of simple polygons. *Computational Geometry*, 3(1):27–35, 1993.

11 Elena Arseneva, Prosenjit Bose, Pilar Cano, Anthony D'Angelo, Vida Dujmovic, Fabrizio Frati, Stefan Langerman, and Alessandra Tappini. Pole Dancing: 3D Morphs for Tree Drawings. In Therese Biedl and Andreas Kerren, editors, *Proceedings of the 26th International Symposium on Graph Drawing and Network Visualization (GD 2018)*, volume 11282 of *LNCS*, pages 371–384. Springer, 2018.

12 Fidel Barrera-Cruz, Penny Haxell, and Anna Lubiw. Morphing Schnyder Drawings of Planar Triangulations. *Discrete and Computational Geometry*, pages 1–24, 2018.

13 Therese Biedl, Anna Lubiw, Mark Petrick, and Michael Spriggs. Morphing Orthogonal Planar Graph Drawings. *ACM Transactions on Algorithms*, 9(4):29:1–29:24, 2013.

14 Clinton Bowen, Stephane Durocher, Maarten Löffler, Anika Rounds, André Schulz, and Csaba D. Tóth. Realization of Simply Connected Polygonal Linkages and Recognition of Unit Disk Contact Trees. In Emilio Di Giacomo and Anna Lubiw, editors, *Proceedings of the 23rd International Symposium on Graph Drawing (GD 2015)*, volume 9411 of *LNCS*, pages 447–459. Springer, 2015.

15 Enno Brehm. 3-Orientations and Schnyder 3-Tree-Decompositions. Master's thesis, Freie Universität Berlin, FB Mathematik und Informatik, 2000. Diploma thesis.

16 Graham R. Brightwell and Edward R. Scheinerman. Representations of Planar Graphs. *SIAM Journal on Discrete Mathematics*, 6(2):214–229, 1993.

17 S. S. Cairns. Deformations of Plane Rectilinear Complexes. *The American Mathematical Monthly*, 51(5):247–252, 1944.

18 Steven Chaplick, Stephen G. Kobourov, and Torsten Ueckerdt. Equilateral L-Contact Graphs. In Andreas Brandstädt, Klaus Jansen, and Rüdiger Reischuk, editors, *Proceedings of the 39th International Worksho on Graph-Theoretic Concepts in Computer Science (WG 2013)*, volume 8165 of *LNCS*, pages 139–151. Springer, 2013.

19 Robert Connelly, Erik D. Demaine, Martin L. Demaine, Sándor P. Fekete, Stefan Langerman, Joseph S. B. Mitchell, Ares Ribó, and Günter Rote. Locked and Unlocked Chains of Planar Shapes. *Discrete & Computational Geometry*, 44(2):439–462, 2010.

20 Giordano Da Lozzo, William E. Devanny, David Eppstein, and Timothy Johnson. Square-Contact Representations of Partial 2-Trees and Triconnected Simply-Nested Graphs. In Yoshio Okamoto and Takeshi Tokuyama, editors, *28th International Symposium on Algorithms and Computation, (ISAAC 2017)*, volume 92 of *LIPIcs*, pages 24:1–24:14. Schloss Dagstuhl - Leibniz-Zentrum für Informatik, 2017.

21 Giordano Da Lozzo, Giuseppe Di Battista, Fabrizio Frati, Maurizio Patrignani, and Vincenzo Roselli. Upward Planar Morphs. In Therese Biedl and Andreas Kerren, editors, *Proceedings of the 26th International Symposium on Graph Drawing and Network Visualization (GD 2018)*, volume 11282 of *LNCS*, pages 92–105. Springer, 2018.

22 Hubert de Fraysseix and Patrice Ossona de Mendez. Representations by Contact and Intersection of Segments. *Algorithmica*, 47(4):453–463, 2007.

23 Hubert de Fraysseix, Patrice Ossona de Mendez, and Pierre Rosenstiehl. On Triangle Contact Graphs. *Combinatorics, Probability, and Computing*, 3(2):233–246, 1994.

24 Erik D. Demaine and Joseph O'Rourke. *Geometric folding algorithms - linkages, origami, polyhedra*. Cambridge University Press, 2007.

25 Stefan Felsner. Lattice Structures from Planar Graphs. *The Electronic Journal of Combinatorics*, 11(1), 2004.

26 Stefan Felsner and Mathew C. Francis. Contact Representations of Planar Graphs with Cubes. In *Proceedings of the 27th Annual Symposium on Computational Geometry (SoCG 2011)*, pages 315–320. ACM, 2011.

27 Stefan Felsner and Günter Rote. On Primal-Dual Circle Representations. In Jeremy T. Fineman and Michael Mitzenmacher, editors, *2nd Symposium on Simplicity in Algorithms (SOSA 2019)*, volume 69 of *OpenAccess Series in Informatics (OASIcs)*, pages 8:1–8:18, Dagstuhl, Germany, 2018. Schloss Dagstuhl–Leibniz-Zentrum fuer Informatik. doi:10.4230/OASIcs.SOSA.2019.8.

28 Stefan Felsner, Hendrik Schrezenmaier, and Raphael Steiner. Equiangular Polygon Contact Representations. In Andreas Brandstädt, Ekkehard Köhler, and Klaus Meer, editors, *Proceedings of the 44th International Workshop on Graph-Theoretic Concepts in Computer Science (WG 2018)*, volume 11159 of *LNCS*, pages 203–215. Springer, 2018.

29 Michael S. Floater and Craig Gotsman. How to morph tilings injectively. *Journal of Computational and Applied Mathematics*, 101(1):117–129, 1999.

30 Daniel Gonçalves, Benjamin Lévêque, and Alexandre Pinlou. Triangle Contact Representations and Duality. *Discrete & Computational Geometry*, 48(1):239–254, 2012.

31 Craig Gotsman and Vitaly Surazhsky. Guaranteed intersection-free polygon morphing. *Computers & Graphics*, 25(1):67–75, 2001.

32 Stephen Kobourov, Torsten Ueckerdt, and Kevin Verbeek. Combinatorial and Geometric Properties of Planar Laman Graphs. In *Proceedings of the 24th annual ACM-SIAM Symposium on Discrete Algorithms (SODA 2013)*, pages 1668–1678. SIAM, 2013.

33 Stephen G. Kobourov and Matthew Landis. Morphing Planar Graphs in Spherical Space. *Journal of Graph Algorithms and Applications*, 12(1):113–127, 2008.

34 Paul Koebe. Kontaktprobleme der Konformen Abbildung. *Berichte über die Verhandlungen der Sächsischen Akademie der Wissenschaften zu Leipzig, Mathematisch-Physikalische Klasse*, 88:141–164, 1936.

35 G. Laman. On Graphs and Rigidity of Plane Skeletal Structures. *Journal of Engineering Mathematics*, 4(4):331–340, 1970.

36 Walter Schnyder. Embedding Planar Graphs on the Grid. In *Proceedings of the 1st ACM-SIAM Symposium on Discrete Algorithms (SODA '90)*, pages 138–148, 1990.

37 Oded Schramm. *Combinatorially Prescribed Packings and Applications to Conformal and Quasiconformal Maps*. PhD thesis, Princeton University, 1990. Modified version: arXiv:0709.0710v1.

38 Hendrik Schrezenmaier. Homothetic Triangle Contact Representations. In Hans L. Bodlaender and Gerhard J. Woeginger, editors, *Proceedings of the 43rd International Workshop on Graph Theoretic Concepts in Computer Science (WG 2017)*, number 10520 in LNCS, pages 425–437, 2017.

39 Vitaly Surazhsky and Craig Gotsman. Controllable morphing of compatible planar triangulations. *ACM Transactions on Graphics*, 20(4):203–231, 2001.

40 Carsten Thomassen. Deformations of Plane Graphs. *Journal of Combinatorial Theory, Series B*, 34(3):244–257, 1983.

41 Carsten Thomassen. Interval representations of planar graphs. *Journal of Combinatorial Theory, Series B*, 40(1):9–20, 1986.

42 W. T. Tutte. How to Draw a Graph. *Proceedings of the London Mathematical Society*, s3-13(1):743–767, 1963.

43 Arthur van Goethem and Kevin Verbeek. Optimal Morphs of Planar Orthogonal Drawings. In Bettina Speckmann and Csaba D. Tóth, editors, *Proceedings of the 34th International Symposium on Computational Geometry (SoCG 2018)*, volume 99 of *LIPIcs*, pages 42:1–42:14. Schloss Dagstuhl–Leibniz-Zentrum für Informatik, 2018.